



Article

Insights into the Subduction of the Ligure-Piemontese Oceanic Basin: New Constraints from the Metamorphism in the Internal Ligurian Units (Northern Apennines, Italy)

Edoardo Sanità ¹ , Maria Di Rosa ¹, Michele Marroni ^{1,2,*} , Francesca Meneghini ^{1,2} and Luca Pandolfi ¹

¹ Dipartimento di Scienze della Terra, Università di Pisa, Via Santa Maria 53, 56126 Pisa, Italy; edoardo.sanita@dst.unipi.it (E.S.); maria.dirosa@unipi.it (M.D.R.); francesca.meneghini@unipi.it (F.M.); luca.pandolfi@unipi.it (L.P.)

² Istituto di Geoscienze e Georisorse, IGG-CNR, Via Moruzzi, 50124 Pisa, Italy

* Correspondence: michele.marroni@unipi.it

Abstract: In the Northern Apennines, the Internal Ligurian Units are considered deformed and metamorphosed fragments of the Ligure-Piemontese oceanic basin. In this paper, we report on the temperature and pressure conditions of the metamorphic peak for four Internal Ligurian Units, estimated using different geothermometers and geobarometers based on the white mica and chlorite compositions. These minerals were formed during the D1 deformation phase in the pre-Oligocene. The results indicate that the Portello and Gottero units are both characterized by metamorphic conditions pertaining to low blueschists facies, while the Colli-Tavarone and Bracco-Val Graveglia Units show a lower metamorphic imprint that produces assemblages of prehnite-pumpellyite facies. The estimated geothermal gradient for the metamorphic peak achieved by the analyzed Internal Ligurian Units during the D1 phase is 7–15 °C/Km, which is indicative of deformation in a subduction setting. Under these conditions, the D1 phase developed in these units as a result of underplating at the base of the accretionary wedge during the closure of the Ligure-Piemontese basin. These data indicate a close geodynamic correlation among the Internal Ligurian Units and the ophiolite-bearing units of the Alps.

Keywords: Northern Apennines; Internal Ligurian Units; high pressure metamorphism; Ligure-Piemontese ocean; subduction



Citation: Sanità, E.; Di Rosa, M.; Marroni, M.; Meneghini, F.; Pandolfi, L. Insights into the Subduction of the Ligure-Piemontese Oceanic Basin: New Constraints from the Metamorphism in the Internal Ligurian Units (Northern Apennines, Italy). *Minerals* **2024**, *14*, 64. <https://doi.org/10.3390/min14010064>

Academic Editor: José Francisco Molina

Received: 30 October 2023
Revised: 29 December 2023
Accepted: 31 December 2023
Published: 4 January 2024



Copyright: © 2024 by the authors. Licensee MDPI, Basel, Switzerland. This article is an open access article distributed under the terms and conditions of the Creative Commons Attribution (CC BY) license (<https://creativecommons.org/licenses/by/4.0/>).

1. Introduction

Ophiolites represent fragments of the oceanic lithosphere preserved as deformed and metamorphosed tectonic units within collisional belts. They can be deformed in different tectonic settings, such as in the subduction zone, during the collision, or along the continental margins by obduction [1]. The reconstruction of their geodynamic settings of deformation is a fundamental step to understand the evolution of collisional belts: the main constraint to this reconstruction is estimating the metamorphic imprint and the pressure (P) and temperature (T) conditions recorded during deformation [2].

Like most of the worldwide collisional belts, the Northern Apennines typically preserves fragments of the oceanic lithosphere consisting of both mantle and crustal sections, including magmatic as well as sedimentary rocks [3–6]. These successions are grouped into the so-called Internal Ligurian (IL) Units that crop out at the top of the Northern Apennines tectonic stack. IL Units are unambiguously interpreted as fragments of the Ligure-Piemontese oceanic basin, the narrow northern branch of the western Tethys basin that opened in the Middle Jurassic between the European and Adria continental margins and was then consumed during a Campanian subduction event that culminated in the Middle to Late Eocene continental collision [7–14]. Because of their relevance in understanding the geodynamic history of the Ligure-Piemontese basin, the IL Units have

been studied in detail to constrain the stratigraphy of the ophiolite sequences and sedimentary covers [3–5,15–19] as well as for the structural features of their pre-Oligocene deformation history [20–29]. However, the available data about their metamorphism are scarce and mainly derived from T estimates of the metamorphic peak from illite and chlorite crystallinity [30–37] and from analyses of the carbonaceous material [31,38,39], whereas the P conditions remain largely undetermined. This is due to the very low kinetics during low- T condition reactions that makes chemical equilibria rarely achieved at the whole rock scale [40], thus hampering the unambiguous constraint of the P – T conditions of metamorphism [41–43]. In addition, it is specifically difficult to assess metamorphic peaks in metasedimentary rocks, since the high content of detrital minerals in relict phases makes effective rock composition largely questionable and unreliable in terms of building isochemical phase diagrams, i.e., pseudosections [44,45]. As a consequence, only an approach based on the combined use of different thermobarometric methods can result in unambiguous estimates.

The lack of reliable data about the metamorphism of the IL Units has hampered an unambiguous definition of the tectonic setting of deformation, which still remains a matter of debate. Most contributions have regarded the IL Units as involved in accretion and subduction with transfer mechanisms to the accretionary wedge ranging from coherent underplating [28] to frontal accretion [4,9,46]. In contrast, some authors [23,26] have regarded the IL Units as located in the trapped crust within the upper plate of the subduction system and consequently deformed only during the inception of the continental collision. Further, other authors have proposed that the deformation of the IL Units is the result of intraoceanic transpressional tectonics during the closure of the Ligure-Piemontese basin [47]. According to these authors, the onset of the transpression occurred during the Late Cretaceous in correspondence with the pre-existing oceanic transform fault.

Recently, Meneghini et al. [48] provided the first evidence of a subduction signature in the IL Units by determining the peak conditions for the IL Units within a narrow area through a quantitative approach based on the white mica–chlorite multi-equilibrium thermobarometry [49]. This result represents the starting point for a complete re-definition of the metamorphism of all the IL Units cropping out in the northwestern side of the Northern Apennines. In this contribution, we report the estimated metamorphic peak in the IL Units by selecting the metapelites from Palombini Shale Fm. belonging to the sedimentary cover of the ophiolite sequence. This formation has been selected because it is present in most of the IL Units and shows the same lithological features everywhere, which minimizes the influence of bulk rock compositional variations. The results are discussed to discriminate the different interpretations proposed for the tectonic setting of the IL Units during the subduction event.

2. Overview of the IL Units

The IL Units crop out extensively in the Northern Apennines from Eastern Liguria, where they are juxtaposed with the Western Alps, through Central Liguria to Southern Tuscany (Figure 1).

Eastern Liguria, along the Lavagna, Sturla, Graveglia and Vara valleys, is the best place to study the IL Units because the stratigraphic successions, even if strongly deformed, are extensively well-exposed. Here, the IL Units consist of a stack of tectonic units (Figure 2a) overlain by the Antola Unit, regarded as belonging to the External Ligurian (EL) Units [50]. The relationships between the Antola and IL Units are sealed by the Early Oligocene conglomerates of the Tertiary Piedmont Basin [27]. The thrust between the Antola and IL Units is affected by a large antiform with a high-angle axial plane, as shown in Figure 2a. This antiform also deforms the overlying deposits of the Tertiary Piedmont Basin [51]. In turn, both the IL and EL Units are thrust during the Miocene over the Subligurian and Tuscan Units. These units, whose succession is derived from the Adria continental margin, consist of Triassic to Tertiary carbonate and siliciclastic deposits topped by foredeep

turbidites, and are well exposed to tectonic windows in the Taro [52] and Aveto valleys in this area [53].

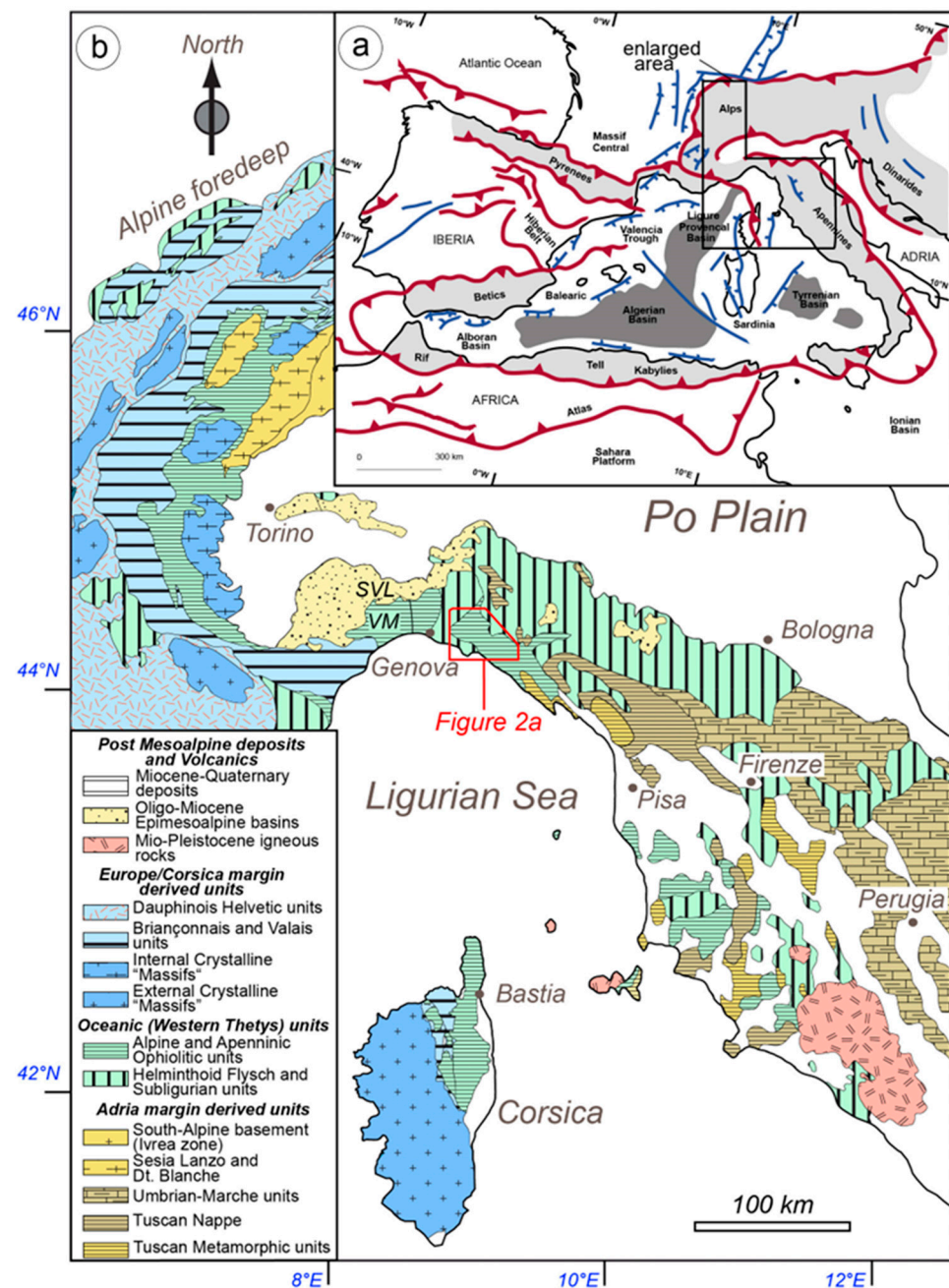
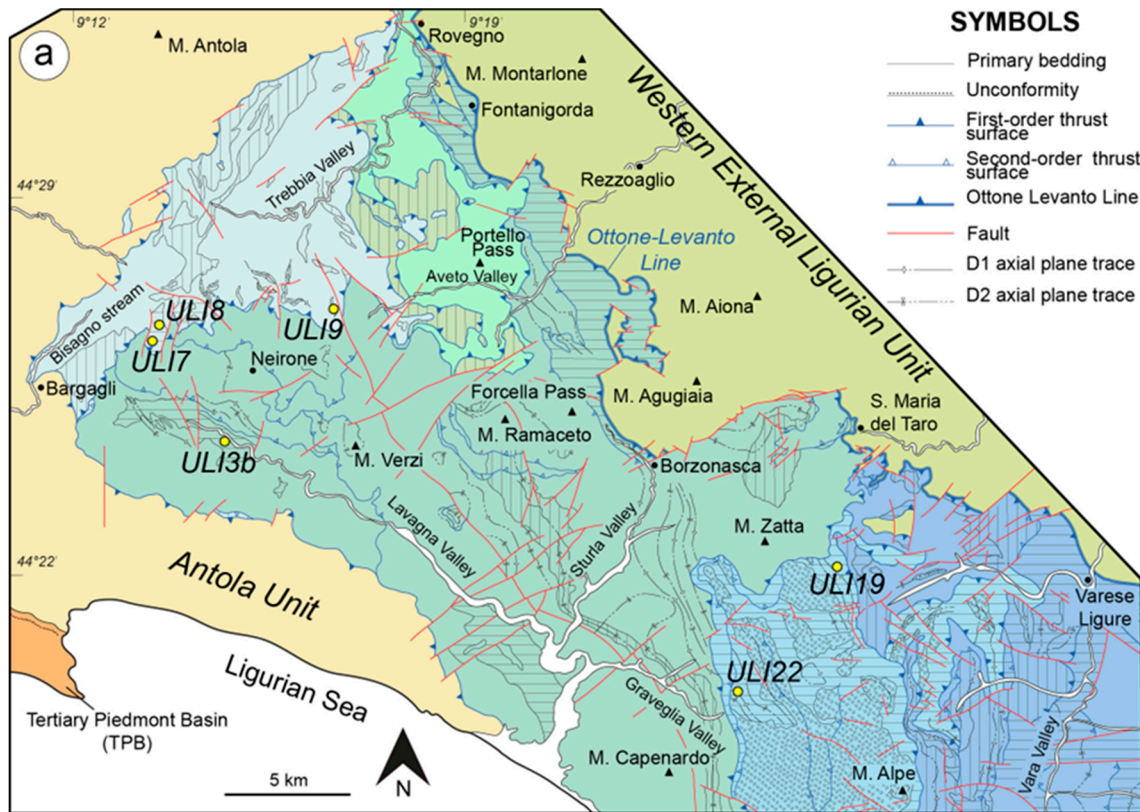


Figure 1. (a) Location of the study area in the western Mediterranean (modified from [27]); (b) Tectonic setting of the Northern Apennines and Alps (redrawn and modified from [54]). SVL: Sestri Voltaggio line; VM: Voltri Massif. Location of Figure 2a is also shown.

The IL Units are bounded by two main, north-south trending and strike-slip fault systems: the Sestri-Voltaggio (Figure 1) and Ottone-Levanto lines (Figure 2a), both regarded as Late Eocene-Early Oligocene in age. The western boundary is represented by the dextral strike-slip Sestri-Voltaggio line, in which the IL Units are juxtaposed against the eclogite-facies ophiolite-bearing units of the Voltri Massif [55], belonging to the Alpine belt [56]. To the east, the Ottone-Levanto line represents the boundary with the EL Units (Figure 2b), which consists of unmetamorphosed successions derived from the ocean-continent transition to the Adria plate margin [27,57].



LEGEND
Internal Ligurian Domain

<p>Portello Unit</p> <ul style="list-style-type: none"> Monte Lavagnola Formation - FVL (Paleocene?) Ronco Formation - ROC (early Campanian) Palombini Shale - PBS (Santoniano-early Campanian) 	<p>Due Ponti Unit</p> <ul style="list-style-type: none"> Canale Formation - FCL (Santonian-early Campanian) 	<p>Bracco-Val Graveglia Unit</p> <ul style="list-style-type: none"> Palombini Shale (Berriasian-Albian) - PBS Ophiolite sequence - Oph (Middle to Late Jurassic), Cherts - DSD and Calpionella Limestone - CL (Callovian-Valanginian)
<p>Vermallo Unit</p> <ul style="list-style-type: none"> Cassingheno Formation - FCS (early Paleocene?) 	<p>Gottero Unit</p> <ul style="list-style-type: none"> Bocco Shale - BCC (early Paleocene) Gottero Sandstone - GOT and Val Lavagna Group - SVL (early Campanian-early Paleocene) Palombini Shale - PBS (Aptian-Santonian) 	<p>Colli-Tavarone Unit</p> <ul style="list-style-type: none"> Tavarone Formation - FCT (early Paleocene) Val Lavagna Group - SVL (early Campanian-early Maastrichtian) Palombini Shale - PBS (Berriasian-Albian)

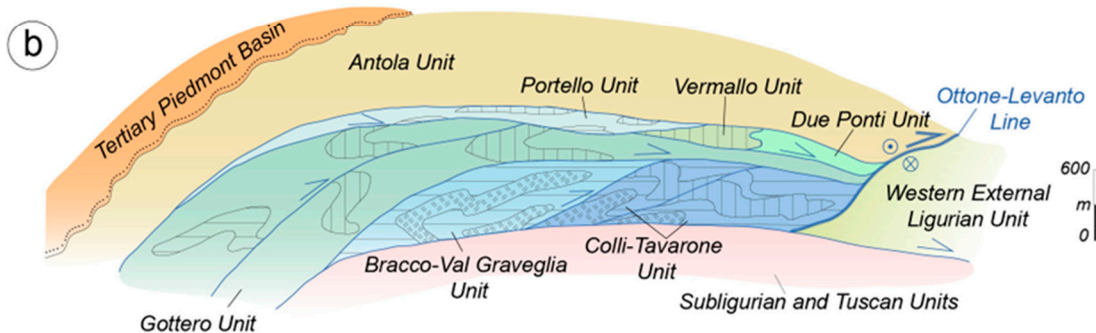


Figure 2. (a) Geological map of the study area. The localization of the sampled areas is shown; (b) Sketch of the stack of units of the Eastern Liguria. In the map, the outcropping area of the ophiolite sequence, the associated deep sea pelagic deposits (i.e., Cherts, Calpionella Limestone and Palombini Shale Fms.), the turbidite deposits (i.e., Lavagna Group, Canale Fm., Ronco Fm., Gottero Sandstone) and the debris flow and slide deposits (i.e., Monte Lavagnola Fm., Cassingheno Fm., Bocco Shale and Tavarone Fm.) are shown. ULI3b, ULI7, ULI8, ULI9 and ULI22 represent the locations of the collected and analyzed samples.

The Ottone-Levanto line displays structural features that indicate deformation with components of top-to-NE thrusting and contemporaneous top-to-SW sinistral/dip-slip shearing [58].

The stack of the IL Units includes, from bottom to the top, the Colli-Tavarone, Bracco-Val Graveglia, Gottero, Vermallo, Due Ponti and Portello Units (Figure 3) [59]. The first two units are characterized by an ophiolite sequence overlain by sedimentary cover, whereas the other units include only segments of the latter. Due to internal thrusting, some IL Units can be subdivided into subunits at the map scale [60].

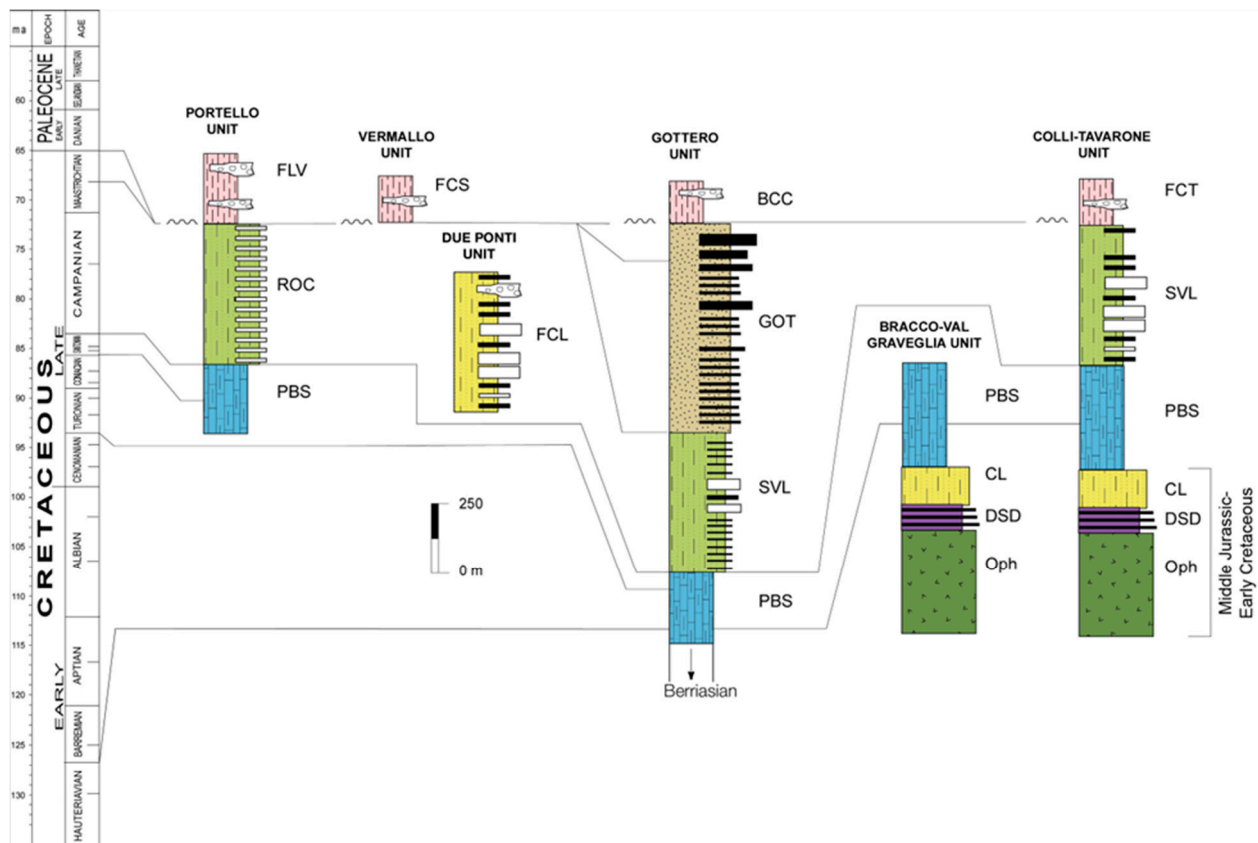


Figure 3. Stratigraphic logs of the IL Units (modified and redrawn from [29]). Oph: Ophiolite sequence; DSD, CL and PBS: deep sea pelagic deposits including Cherts, Calpionella Limestone and Palombini Shale Fms., respectively; SVL, FCL, ROC and GOT: turbidite deposits including Lavagna Group, Canale Fm., Ronco Fm., Gottero Sandstone, respectively; FLV, FCS, BCC and FCT: debris flow and slide deposits including Monte Lavagnola Fm., Cassinighe Fm., Bocco Shale and Tavarone Fm., respectively.

2.1. Stratigraphic Setting

All the IL Units are derived from the lithosphere belonging to the Ligure-Piemontese ocean and are made up by the same stratigraphic sequence or by a section of it. So, a complete stratigraphic log can be fully reconstructed only by the integration of data available from the different tectonic units (Figure 3).

At its base, this cumulative log includes a Middle-to-Late Jurassic ophiolite sequence covered by a thick sedimentary cover ranging in age from Late Jurassic to Early Paleocene. The ophiolite sequence is characterized by a 500–600 m thick basement consisting of serpentinized mantle lherzolite intruded by small gabbro bodies. The basement is covered by a volcano-sedimentary complex, up to 300–400 m thick, that consists of pillow lavas and massive basaltic flows interfingering with ophiolite breccias and cherts. The ophiolite sequence [7] shows a transition to deep-sea pelagic deposits sedimented in a basin plain depositional setting below the CCD (calcite compensation depth) with a very low rate of sedimentation [27].

The Palombini Shale Fm. is the youngest and the most representative formation of this deep-sea pelagic sequence and is recognized in all these units, with the only exceptions represented by the Vermallo and Due Ponti Units. The Palombini Shale Fm. grades upward to turbiditic deposits ranging from the Campanian to Early Paleocene age. These deposits belong to a complex turbidite fan system that includes mixed siliciclastic-carbonatic and siliciclastic turbidites supplied by the European continental margin [61]. These turbidites are regarded as tectonically controlled deposits sedimented in a trench system developed since the Campanian [62]. The youngest formation of the IL Units is represented by the Early Paleocene debris flow and slide deposits lying unconformably on top of all the older formations in the Gottero, Portello and Colli-Tavarone Units. This formation has been interpreted as trench deposits related to an event involving frontal tectonic erosion of the accretionary wedge slope [29].

2.2. Pre-Oligocene Deformation History

The IL Units are polydeformed and show evidence of multiple events of veining, folding and thrusting. These events are grouped in two phases, D1 and D2, both of which developed in the pre-Oligocene. Each phase includes a set of progressive deformation steps that are all coherent from a structural point of view and resulting from the same tectonic process. Due to the lack of geochronological constraints, the age of the deformation phases has been constrained by the IL Units-derived clasts found within the Early Oligocene conglomerates of the Tertiary Piedmont Basin. These clasts, set in an undeformed matrix, display two deformation phases like those detected in the IL Units [63].

The most complete description of these two deformation phases was provided by [28] for the Gottero Unit, but the same deformation history has been identified in all the other IL Units such as the Bracco-Val Graveglia [25] and Colli-Tavarone [16] or the Portello, Vermallo and Due Ponti Units [27].

In all the IL Units, the D1 phase is the most pervasive in the field, and it consists of a sequence of deformations connected to the metamorphic peak. The D1 phase has been divided into three sub-phases, respectively, reported as the D1a, D1b and D1c sub-phases according to Meneghini et al. [28]. According to Hoogerduijn Strating and Van Wamel [25] and Marroni and Meccheri [16], the same subdivision can be proposed for the deformation history reconstructed in the Bracco-Val Graveglia and Colli-Tavarone Units.

During the D1a sub-phase, only a network of veins is developed before any folding or thrusting phase. These veins might be interpreted as small-scale fractures representing conduits for fluid migration in partially lithified sediments, probably during stress-controlled compaction. The D1b sub-phase is characterized by strongly non-cylindrical, isoclinal D1 folds that deform both bedding and pre-existing veins. The D1 folds show thickened hinge zones, while the limbs are generally affected by boudinage and necking. The facing of the D1 folds is consistently toward NW (Figure 4a,b). Associated with the D1b sub-phase is a strongly developed S1 axial-plane foliation that is not transposed by the subsequent deformations. In the metapelites, the S1 foliation can be classified as slaty cleavage being characterized by elongate quartz-albite-mica aggregates surrounded by aligned fine-grained phyllosilicates. A metamorphic mineral assemblage of white mica + chlorite + quartz + calcite + albite + Fe-oxides has been detected in the metapelites (Figure 4a,b). Pressures shadows around detrital minerals are well developed, showing infillings of fibrous minerals such as quartz, phyllosilicates and calcite. The subsequent D1c sub-phase is characterized by the development of brittle shear zones consisting of m-thick foliated cataclasites generally parallel to the S1 foliation. Their microscale structures, as asymmetric recrystallized tails around detrital minerals, suggest a top-to-NW sense of shear.

The D2 phase is also the result of progressive deformation steps. The D2a sub-phase is characterized by recumbent asymmetric folds with sub-horizontal axes and flat-lying axial planes. These folds show an approximately parallel geometry with sub-rounded to rounded hinges. The facing of the D2 folds is everywhere towards the E. The D2 folds everywhere deform the S1 foliation as well as the D1 folds, thus producing a type 3 interference pattern.

The axial plane foliation of the D2 folds is represented by a crenulation cleavage ranging from discrete to zonal types [64]. The S2 foliation is defined by cleavage domains showing a gradual transition to microlithons, without any metamorphic recrystallization. The D2 folds are systematically associated with low-angle, normal/dip-slip cataclastic shear zones as detected by the shear sense criteria. The subsequent D2b sub-phase is represented by high-angle normal faulting that cuts all the pre-existing structures.

According to [28], the boundaries between the different IL Units as well as the internal imbrication of the units into subunits consist of cataclastic shear zones developed during either the D1 (sub-phase D1c) or the D2 phase (sub-phase D2a). For instance, the subunits of the Gottero Unit are coupled at the end of the D1 phase, as recognized in the Sturla Valley by [58]. Similarly, the shear zones responsible for the internal imbrication of the Colli-Tavarone Unit are deformed by the D2 folds, as is the boundary between this unit and the Bracco-Val Graveglia Unit [16]. Other boundaries, as those between the Gottero and the Bracco-Val Graveglia or the Colli-Tavarone Units, are deformed only by the large antiform that also affected the Antola Unit and the Tertiary Piedmont Basin. All these unit-bounding shear zones, occurring as flat-lying surfaces, are therefore regarded as having developed during the D2 phase. This timing of deformation has also been proposed for the boundary between the Gottero and Portello as well as the Vermallo and Due Ponti Units.

Overall, the IL Units consist of an assemblage of tectonic units, derived from the same ophiolite sequence, whose coupling occurred after the metamorphic peak, i.e., after the D1b sub-phase.

3. Previous Studies on the Metamorphism of IL Units

The metamorphism of the IL Units from Central Liguria, i.e., the Cravasco-Voltaggio and Mt. Figogna Units, is well known owing to the occurrence of metabasalts and metagabbros with a metamorphic peak produced under low-blueschist facies P - T conditions [65,66]. In contrast, the peak metamorphism in the IL Units of Eastern Liguria is less constrained, especially for the P estimates. The first data about these units were provided by [30], who determined the crystallinity and polytypism of illite, i.e., the Kubler Index, in different formations. These authors studied samples collected from turbidite deposits in the Gottero Unit as well as samples collected from pelagic deposits in the Bracco-Val Graveglia Unit. Reutter et al. [38] determined the vitrinite reflectance, from which the metamorphic grade in the turbidites cropping out in the area between the Lavagna and Sturla valleys was obtained. Bonazzi et al. [31] provided both illite crystallinity and vitrinite reflectance data for a wide range of lithologies belonging to the Gottero and Bracco-Val Graveglia Units. The results obtained by [31] were subsequently confirmed for the Bracco-Val Graveglia Unit by [67] who analyzed prehnite and pumpellyite formed in the basalts during the orogenic event. Further data related to the metamorphism of the IL Units were provided by [33]. Subsequently, refs. [32,34] reported additional data using the same methods. However, all these studies provide ranges of T conditions but do not offer quantifications of the metamorphic peak conditions. Only [35,36] provided estimates of P and T values by using Illt and Chl crystallinity and the Illt b0 parameter measured in samples of Palombini Shale Fm. collected from some IL Units in Liguria. The P values estimated using the Illt b0 parameter are, however, largely approximates, as they were in fact obtained by comparison with the same parameters detected in the Palombini Shale Fm. of the ophiolite-bearing units cropping out in the Sestri-Voltaggio area, where P was determined by the metamorphic mineral assemblage in metabasites. Further insight was provided by [68] who obtained Paleozoic ages from analyses of the fission tracks from zircons collected in the Gottero Sandstone Fm. of the Monte Ramaceto and Monte Zatta outcrops. Findings suggest that the T of the metamorphism did not exceed the T proposed for the annealing of fission tracks [69]. In [28], the T was estimated qualitatively for the metamorphic peak in the Palombini Shale Fm. from the Forcella Pass by the twin types in calcite fibers recrystallized during peak metamorphism [70,71]. Lastly, [39] provided two T estimates for the Palombini

Shale Fm. from the Gottero Unit using the Raman Spectroscopy of Carbonaceous Material (RSCM) method.

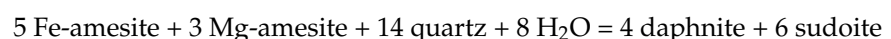
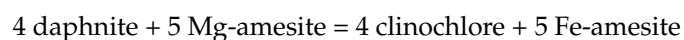
4. Sampling Strategy and Methods

The metamorphic conditions of the IL Units were estimated from samples in the Palombini Shale Fm. based on the metamorphic paragenesis grown along the S1 axial plane foliation during the D1b phase (Figure 4a,b). This formation is made up of an alternance of layers of meta-limestones, shales and coarse-to-medium meta-siltstones that repeat homogeneously along the entire formation thickness in all the different units. The homogenous lithology of the Palombini Shale Fm. and its occurrence in most of the IL Units make this formation the best candidate on which the quantification of the P , T condition of all the IL Units can be attempted. The analyzed samples are meta-siltstones collected from where the S1 foliation is best preserved, i.e., along the limbs of the D2 folds and far from the cataclastic shear zones. The sampling areas are shown in Figure 2a. The samples are constituted by flakes of detrital white mica (up to 70 μm in length), chlorite (30–50 μm), quartz (20–30 μm), albite (10–20 μm), and minor titanite (Ttn) and K-feldspar (5–10 μm) dragged into a phyllosilicate-bearing matrix (<10 μm , Figure 4c,d). The metamorphic paragenesis made of the chlorite + white mica + quartz + albite \pm K-feldspar \pm calcite set that defines S1 is recognizable in all the samples (Figure 4c,d). S1 foliation is well developed, and the recrystallized domains do not exceed 5–10 μm in thickness (Figure 4c,e,f). Mineral chemistry coupled with micro-texture are the criteria used to distinguish the detrital chlorite and white mica grains from the neo-formed ones. In the latter, a further selection based on the relationships between chlorite and white mica grains grown in the same micro-domain and showing clear equilibrium relationships was performed. Generally, the detrital grains (Figure 4f) show frayed edges and slight core-to-rim chemical zoning, unlike the syn-metamorphic ones.

Spot analyses and quantitative maps of compositions were acquired using the Electron Probe Microanalyser (EPMA), following the procedure by [72]. The XMapTools [73] software was used for sampling in the micro-areas and applying classical thermometers [74–76] and the geobarometer from [77]. The range of P (GPa) and T ($^{\circ}\text{C}$) in which chlorite and white mica are in equilibrium was verified using different methods [78,79]. The outcoming P – T conditions of chlorite-white mica couples defining the S1 foliation were then estimated by using the chlorite-phengite-quartz-water [80] method. The analyses show that the total (oxides%) of white mica is higher than the standard: these high values are attributable to an overlap of the beam, which is derived from the stacking of the white mica beam with those of other mineral phases such as chlorite, plagioclase or quartz. Such overlapping of beams can hardly be avoided. The eventual low K_2O values observed in white mica is attributable to sample alteration, and we attempted to minimize this problem by sampling only the freshest available portions.

To test our results, the T values for the Gottero, Portello, Colli-Tavarone and Bracco-Val Graveglia Units obtained in this work were compared using four different geothermometers.

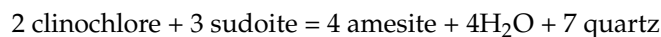
The chlorite-quartz-water method [78] provided the T related to a single analysis of the base of the content of the chlorite end-members and modeled with the following reactions:



These reactions were calculated assuming an initial value of water activity ($a_{\text{H}_2\text{O}}$). If samples lack carbonates, $a_{\text{H}_2\text{O}}$ is assumed to be 1.0. An $a_{\text{H}_2\text{O}}$ value of 0.8 was used for the samples that contain calcite, since the non-water part needs to be modelled into the fluid budget [81]. Only the analyses for which the reactions reached the equilibrium conditions in an interval of 30 $^{\circ}\text{C}$ were considered. Together with the T , the percentage of Fe^{3+} values associated with each single analysis is reported. Calculations were performed at different starting P values (see Supplementary Material), so as to cover a wide range

of pressure conditions of metamorphic facies from the prehnite-pumpellyite (0.1 GPa) up to the low/medium blueschist (1.0 GPa). The P value at which the Fe^{3+} becomes homogeneous for a larger number of chlorite analyses was chosen as the best value, and consequently the T range associated with that P value was the interval chosen as the most reliable [82].

The thermometer for di-trioctahedral chlorite [75] is based on four independent end-members which follow the reaction:



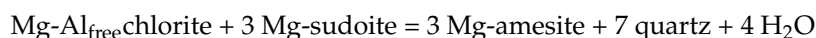
This reaction is appropriate for meta-sediments reaching peak conditions at T lower than 400 °C. Since the geothermometer works only by setting a Fe^{3+} percentage, in this work, we adopted the average Fe^{3+} value calculated for each sample using the chlorite-quartz-water method.

T results were also compared using Cathelineau's geothermometer [74]. This method is based on the linear relation existing between the Al^{VI} content in the tetrahedral site of chlorite and T using the following formula:

$$T \text{ (}^\circ\text{C)} = -61.92 + 32.98 (\text{Al}^{\text{VI}})$$

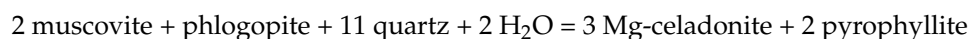
Cathelineau's geothermometer provides reliable results between 150 and 300 °C and when the initial Fe^{3+} percentage is selected based on the results of the chlorite-quartz-water method.

The last geothermometer used in this work is that by Bourdelle et al. [76], specifically for low T (<350 °C) and P (<0.4 GPa) conditions. This method is modelled based on the solid solutions among six end-members of chlorite, which are modelled using the following reaction:



This geothermometer was used for its independence from Fe^{3+} content [76].

P conditions were calculated using the phengite-quartz-water method [79] and Massonne and Schreyer's geobarometer [77]. The former is based on the dehydration of white mica, which is P and T dependent and is modelled by the following reaction:



The results are represented by a line along which the interlayer water content (in the A-site) varies by increasing P and T . In this study, the value of interlayer water was chosen by considering the consistency observed in the white mica analysis of each sample, according to many studies [81]. The range of P relating to each sample was then identified by choosing the most consistent interlayered water content among the individual analyses, setting the T value and a percentage of Fe^{3+} a priori. These two latter values were set based on the results of the chlorite-quartz-water method.

The geobarometer by Massonne and Schreyer [77] was adopted for a comparison with the results obtained using the phengite-quartz-water method. This popular geobarometer is essentially based on the linear increase of Si content (atoms per formula unit, a.p.f.u.) with P . In our sample, this geobarometer was applied to the same micro-areas selected on the micro-maps sampled for the phengite-quartz-water method. As indicated by the authors who created the barometer, for all samples in which the mineral assemblage of the samples did not coincide with that for which the barometer is optimized, the P values obtained were considered as representative of the minimum P values reached during the peak metamorphism in that tectonic unit [77,83].

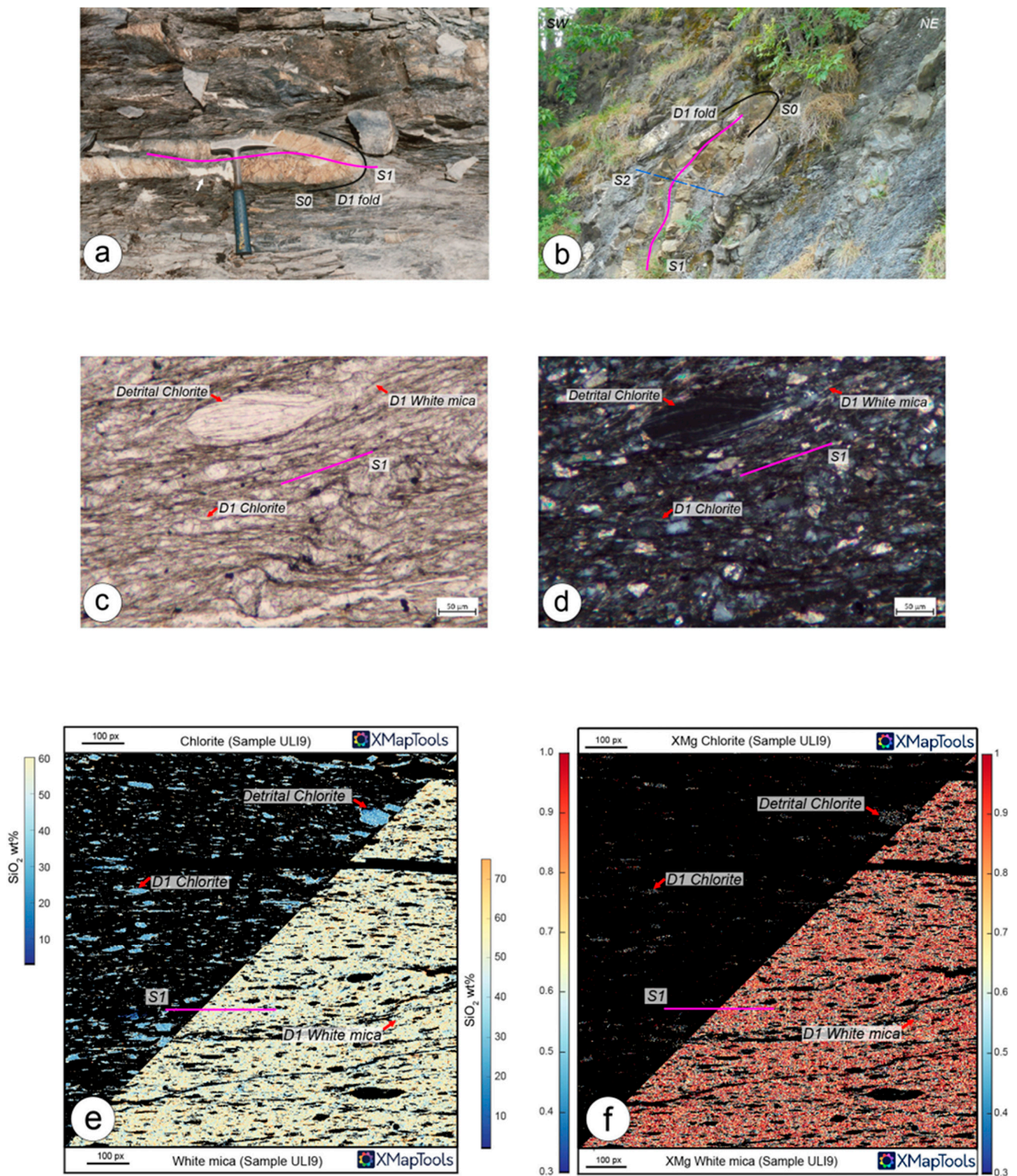
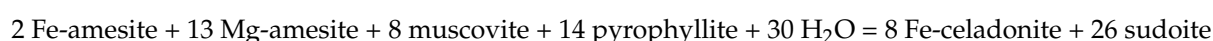
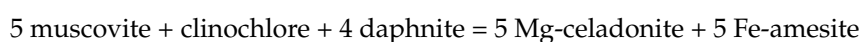
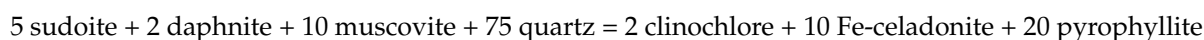
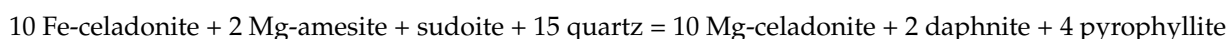
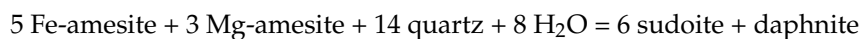
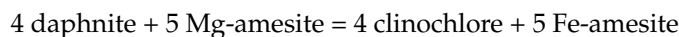


Figure 4. The D1 phase registered by the Palombini Shale Fm. from meso- to micro-scale. D1 mesofold (a,b) in the Gottero Unit. The S1 foliation in thin section (sample ULI9), Portello Unit, at (c) plane-polarized light and (d) cross-polarized light. EPMA micro-map of sample ULI9, showing the distribution of (e) SiO₂ (wt%) and (f) XMg content in Chl and Wm. S0: primary bedding; S1: D1 phase-related axial plane foliation; S2: D2 phase-related axial plane foliation. Mineral abbreviation after [84].

A numerical approach based on the thermodynamic equilibrium of chlorite-white mica couples defining the same microstructure was used to estimate the P – T peak conditions of the samples from the IL Units. The chlorite-phengite-quartz-water method [80] allowed us to define the P – T equilibria based on the following:



Only the equilibria of chlorite and white mica that fit with the P – T ranges and were estimated using the chlorite-quartz-water and the phengite-quartz-water methods were considered in this work. The equilibrium tolerance for each single equilibrium was set to 1 kJ for all samples except for ULI9, which was raised to 5 kJ for the sake of better statistics. According to Vidal and Parra [80], the final error associated with this approach is 30 °C and 0.2 GPa for T and P , respectively.

5. Mineral Chemistry

5.1. Chlorite

The mineral chemistry of chlorite defining S1 was determined from six samples of Palombini Shale Fm. from the Gottero, Portello, Colli-Tavarone and Bracco-Val Graveglia Units. The sample from the Gottero Unit (sample ULI3b) is characterized by XMg ranging between 0.35 and 0.47, Al (Altot = M2 + M3 + M4) content that varies from 2.25 to 2.98 a.p.f.u. and Si values ranging between 2.75 and 2.99 a.p.f.u. (Figures 4f and 5a, see also Supplementary Material for all of the range values reported in the text). Al in chlorite from samples in the Portello Unit (ULI7, ULI8 and ULI9) is included between 2.52 and 3.17 a.p.f.u. (Figure 5a). The Si values range between 2.65 and 2.98 a.p.f.u., whereas the XMg values (0.34–0.73) tend to be higher than those of the Gottero Unit. The sample from the Colli-Tavarone Unit (ULI19) shows the lowest XMg range of all the samples studied (0.26–0.41), while the Al and Si content fits with the trend observed in the other samples (ca. 2.72–3.01 and 2.69–2.77 a.p.f.u., respectively).

The sample from the Bracco-Val Graveglia Unit (ULI22) has Si and Al content of 2.60–2.74 and 2.61–3.14 a.p.f.u., respectively and XMg of 0.34–0.46. All the samples tend to be characterized by $\text{Fe}^{2+} + \text{Mg}^{2+}$ ranging between 3.5 and 4.5 a.p.f.u. resulting in an end-member proportion that tends towards clinochlore/daphnite (Figure 5a). The Si content of all the samples implies that they have more than 50% of the amesite component.

5.2. White Mica

Together with chlorite, along the S1 foliation, neoblasts of white mica also occur (Figure 5b). The lowest Si content is found in white mica occurring in samples from the Bracco-Val Graveglia Unit (3.06–3.28 a.p.f.u.), Colli-Tavarone Unit (3.13–3.31 a.p.f.u.) and Gottero Unit (3.21–3.36 a.p.f.u.). The highest contents of Si are reported in the Portello Unit (up to 3.53 a.p.f.u., Figure 5b). The Bracco-Val Graveglia and Portello Units show more variable XMg ranges (0.20–0.72 and 0.25–0.75, respectively) than the Colli-Tavarone and Gottero Units (0.43–0.61 and 0.11–0.52, respectively). K in white mica ranges between 0.40 and 0.89 a.p.f.u. in all the samples studied (Figure 5b, see Supplementary Material). On average, the white mica studied has a high content of Al_2O_3 , which shifts all analyses towards the muscovite end-member.

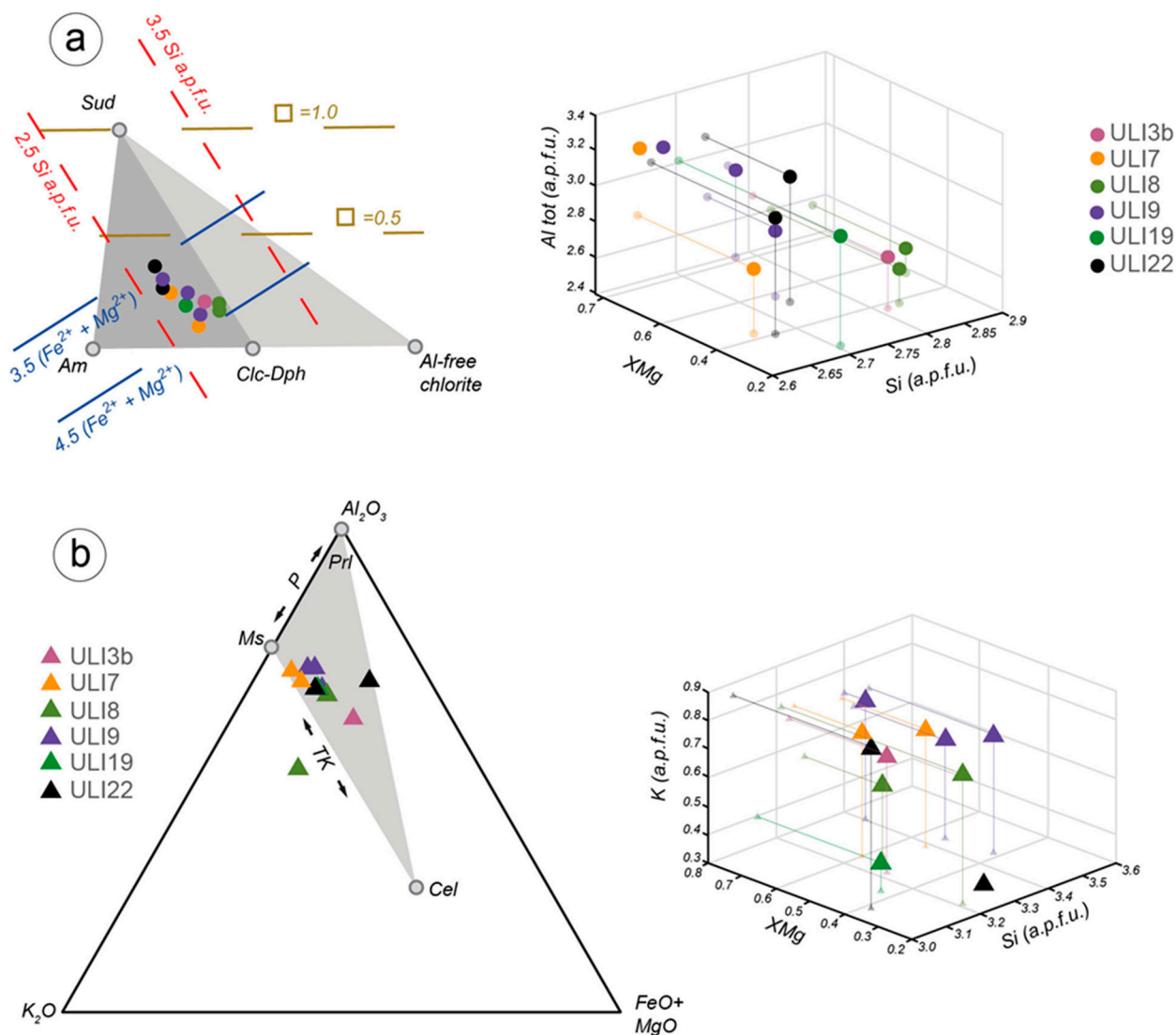


Figure 5. Mineral chemistry of Chl and Wm in the samples studied in this work. (a) Chl end-member proportion (triangular plot according to [85])—squares indicate the value of octahedral vacancy) with 3D diagram showing Si, XMg and Al content. (b) Wm end-member proportion (taken from [80]) with 3D diagram showing Si, XMg and K content. The plots refer to examples of Chl-Wm couples for each sample that reach the equilibrium condition at the lowest Gibbs free energy. See the Supplementary Material for an exhaustive summary table, where the mineral chemistry of white mica and chlorite used to estimate the *P–T* conditions is reported.

6. *P–T* Estimates

The chlorite-quartz-water method [78] was applied six times on each sample considering different starting *P* (see Table S3 of the Supplementary Material). All the calculations were performed after setting the aH₂O to 0.8. In the Gottero Unit, *T* ranged between 190 and 320 °C, whereas in the Portello Unit, *T* showed a wider range but never exceeded 350 °C. For the samples of Colli-Tavarone and Bracco-Val Graveglia Units, *T* ranges of 170–330 °C and 230–330 °C were respectively estimated (Figure 6).

The geothermometer for di-trioctahedral chlorite [75] was applied to all the samples. The *T* ranges estimated were similar to but lower than those estimated using the chlorite-quartz-water method. In ULI7 (i.e., the Portello Unit), this method allowed for better constraining of the *T* range of the metamorphic peak to values higher than 200 °C.

Cathelineau's calibration [74] produced a range of T that covered the interval of 100–350 °C in all the samples. This range was consistently broadened towards high T in samples where higher values were identified with other thermometers, such as ULI7 (ca. 370 °C, Figure 6).

The application of the Bourdelle et al. geothermometer [76] provided results similar to the T range estimated from previous methods, even if a systematic drift towards low T is observed in all samples (Figure 6). This is probably due to the P range that our samples are expected to cover (0.4–1.2 GPa), which tends to be higher than those for which Bourdelle's method is optimized (<0.4 GPa).

P estimates were obtained by comparing the phengite-quartz-water method [79] with Massonne and Schreyer's geobarometer [77] (see Figure 6 and Figure S1 of the Supplementary Material).

Samples from the Gottero and Portello Units show the highest P (0.8–1.0 and 0.4–1.1 GPa, respectively). The Colli-Tavarone and Bracco-Val Graveglia Units are instead characterized by lower P , which are 0.4–0.8 GPa and 0.1–0.6 GPa, respectively. The Massonne and Schreyer's geobarometer [77] provided P that overlap these ranges of pressure (Figure 6).

The P – T equilibrium conditions of selected chlorite-white mica couples were defined using the chlorite-phengite-quartz-water method and considering the P – T ranges defined with the other geothermometers and geobarometers. The Gottero Unit reached the metamorphic peak at 200–230 °C and 0.8–1.0 GPa.

The samples of the Portello Unit are all coherently characterized by P – T conditions of 220–310 °C and 0.7–1.0 GPa. The Colli-Tavarone and Bracco-Val Graveglia Units are both characterized by lower P – T conditions, which are 0.4–0.6 GPa /170–250 °C and 0.4–0.5 GPa/230–270 °C, respectively (Figure 6).

7. Discussion

7.1. Estimation of P – T Metamorphic Conditions

In this contribution, the metamorphic conditions of four tectonic units of the IL Units from Eastern Liguria (i.e., the Gottero, Portello, Colli-Tavarone and Bracco-Val Graveglia Units) are determined. These estimates are based on samples from the Palombini Shale Fm. showing S1 defined by neo-crystalline chlorite and white mica.

These P – T conditions can be associated with the metamorphic peak that occurred during the D1 event of deformation in the IL Units at different P – T conditions. The estimates allow for identifying two groups of units (Figure 7). The Bracco-Val Graveglia and Colli-Tavarone Units recorded the lowest P – T peak conditions. The lowest T (170–250 °C) was registered by the sample ULI19, from the Colli-Tavarone Unit, whereas the sample ULI22, collected in the Bracco-Val Graveglia Unit, reached a slightly higher T (230–270 °C).

The P calculated for these two units is comparable, being estimated as ranging from 0.4 to 0.6 GPa. So, for these two units, the metamorphic peak registered during the D1 phase can be regarded as having occurred at P – T conditions pertaining to prehnite-pumpellyite facies (Figure 7).

The second group is represented by the Gottero and Portello Units where different P – T peak conditions were registered. The samples from the Gottero and Portello Units show peak T values (200–300 °C) that are slightly different from those of the Bracco-Val Graveglia and Colli-Tavarone Units, but higher P values. These values are estimated as 0.8–1.0 GPa for the Gottero Unit and as 0.7–1.0 GPa for the Portello Unit. The estimated P – T conditions indicate that the second group of IL Units were deformed under low blueschist facies conditions. The values detected for the Gottero Unit are coherent with the values estimated by Meneghini et al. [48] for the same unit, even if the samples analyzed by these authors were derived from a different subunit. These data, which were performed on the Palombini Shale Fm. using the same methodology as in this contribution, indicate a P condition from 0.6 to 0.9 GPa. By comparing the P – T estimates of Meneghini et al. [48] with the dataset presented in this work, similar metamorphic peak conditions for the samples of the Gottero Unit and Portello Unit can be observed (Figure 7).

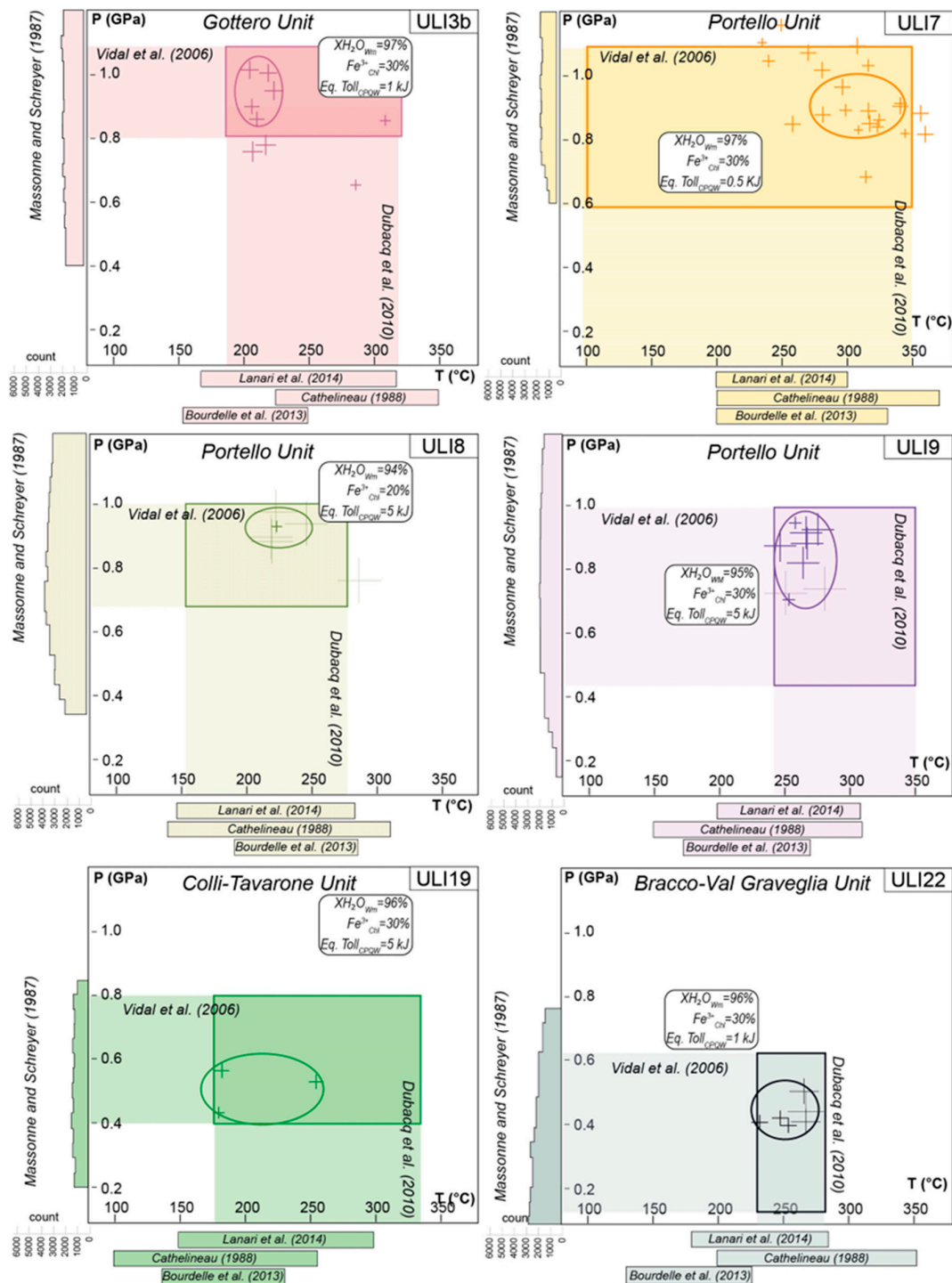


Figure 6. P/T diagrams showing the results of the thermobarometric estimation performed on the samples from the IL Units. Colored boxes in the P/T space indicate the areas constrained with chlorite-quartz-water and phengite-quartz-water methods. Colored crosses indicate the P–T equilibrium conditions of single selected Chl–Wm couples obtained using the chlorite-phengite-quartz-water multi-equilibrium method. Along the X and Y axes, the results of the applied geothermobarometer used to test the reliability of our estimates are reported. In the inset, the estimated interlayer water content in Wm, Fe^{3+}_{Chl} percentage and equilibrium tolerance (used with the chlorite-phengite-quartz-water method, CPQW) values for each sample are reported. The ellipses indicate the selected P–T conditions for each investigated sample [74–76,78,79].

The quantification of the P – T conditions allows us to better define the characteristics of the IL Units stack that can be now described as made of two groups of units deformed during the same D1 phase but at different metamorphic conditions, with the Gottero and Portello Units structured at a deeper structural level than the Colli-Tavarone and Bracco-Val Graveglia Units. Uncommonly, the units with higher metamorphic imprints are now stacked over those with lower metamorphic conditions, with a P gap in between.

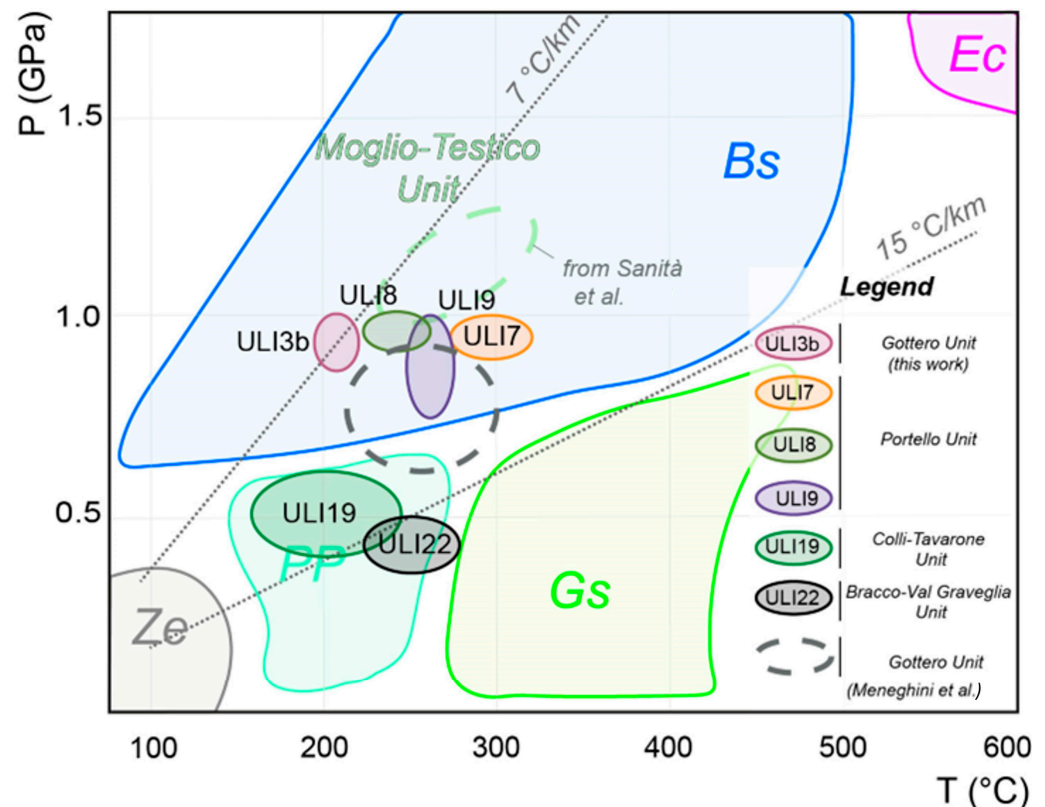


Figure 7. P – T metamorphic conditions of the IL Units (colored ellipsoids) obtained in this work. Ellipsoids include only the Chl-Wm couples in equilibrium that form clusters in the P/T space (i.e., crosses shown in Figure 6). Other samples from the IL Units (i.e., [48,82]) are also plotted. The diagram was redrawn and modified from [86] and quoted references.

7.2. Comparison with Previous Estimates of P – T Conditions

The results of this study can be compared with previously published contributions on the IL Units of Eastern Liguria (Table 1). As previously mentioned, these studies mainly concern the estimation of T using Illt and chlorite crystallinity [30,32–35], carbonaceous material analysis [38], or both methodologies applied together [31,33]. In contrast, only the semiquantitative estimates of P using the Illt b0 parameter are available [35,36].

Regarding the estimation of T using Illt crystallinity, for the diagenesis/anchizone and the anchizone/epizone boundaries, all authors referred to Kübler's index values of $\Delta 2\theta = 0.42^\circ$ and $\Delta 2\theta = 0.25^\circ$ [87], respectively ([88] and [89] for more details on anchizone and epizone metamorphism). These boundaries are regarded by [90] and by [86] as corresponding to T of 200–250 °C and 300–350 °C, respectively. Considering these boundaries, the T data obtained in this study confirm the results reported in [32–36] that indicate a T within the anchizone field. The data by Leoni et al. [36] on peak metamorphism indicate a T of 210–270 °C for the Gottero Unit and a T of 160–210 °C for the Bracco-Val Graveglia Unit.

Table 1. Summary table of the metamorphic imprint based on the T estimates from previous authors. Each number between brackets indicates the used method to estimate T . No data are available for the Portello and Due Ponti Units.

Authors	Gottero Unit	Bracco-Val Graveglia Unit	Colli-Tavarone Unit
Venturelli and Frey, 1979 (1)	anchizone	anchizone	
Reutter et al. 1980 (2)	diagenesis/anchizone		
Bonazzi et al., 1987 (1,2)	anchizone/epizone	anchizone	
Lucchetti et al. (1990)		prehnite-pumpellyite facies	
Reinhardt, 1991 (1,2)	anchizone		
Molli et al., 1992 (1,3)	anchizone		
Ducci et al., 1995 (1,3)	anchizone		
Leoni et al., 1992 (1,3)		anchizone	
Leoni et al., 1996 (1,3)	anchizone	anchizone	anchizone
Balestrieri et al., 1996 (4)	T range of 270–350 °C		
Marroni et al., 2004 (5)	T greater than 200 °C		
Malavieille et al., 2016 (6)	$T = 253$ °C		

1: illite crystallinity; 2: vitrinite reflectance; 3: chlorite crystallinity; 4: Fission tracks annealing; 5: twin types in Cc fibers; 6: RSCM.

The same authors also provided quantitative data about the Colli-Tavarone Unit, where the peak conditions are characterized by a T of 200–250 °C. In contrast, the values reported by [31] indicate a wider range of T that produced grades ranging from anchizone to epizone. The occurrence of samples with an epizone metamorphic imprint indicate T conditions higher than those estimated in this study. This discrepancy is probably due to the fact that [31] analyzed samples from different lithologies and in different structural positions, such as shear zones and/or fold limbs—features that can influence the Illt crystallinity values [91].

A comparison can also be made between our data and those by [38] based on vitrinite reflectance analyses of turbidite deposits from the Gottero Unit. The collected data indicate that most T values reflect diagenesis/anchizone metamorphic conditions, with R_m values greater than 4%. The first data concur with our results, but the second are puzzling. However, the occurrence of the diagenesis was not confirmed by the subsequent study on the Gottero Unit by [33], involving vitrinite reflectance and Illt crystallinity and that has shown prevailing anchizone conditions. These data, as well as those resulting from zircon fission tracks [68], calcite twinning [28] and RSCM methods [39], are in agreement with the results obtained in this study.

In contrast, the available P estimates are only semiquantitative, having obtained Illt b_0 values [35,36] of 0.4 GPa for the Gottero Unit, 0.2–0.3 GPa for the Bracco-Val Graveglia Unit and 0.2–0.3 GPa for the Colli-Tavarone Unit. They confirm the difference in P between the Gottero Unit and the coupled Bracco-Val Graveglia and Colli-Tavarone Units, as assessed in this contribution. A further qualitative evaluation of P has been provided by [67] that recognized an orogenic-related prehnite-pumpellyite assemblage in the basalts of the Bracco-Val Graveglia Unit.

Overall, the data provided in this paper are coherent with most T estimates provided in previous published contributions, mainly the most recent ones. In contrast, the P values estimated in this study are the first quantitative data provided for these units.

7.3. Geodynamic Implications for the Closure of the Ligure-Piemontese Oceanic Basin

Based on the data collected in this paper, the P – T conditions estimated for all the IL Units indicate that the metamorphic peak was acquired at a depth of about 13–35 km in a setting characterized by a geothermal gradient of about 7–15 °C/Km (Figure 7). This is the

crucial result of this study because it allows us to discard some of the previous geodynamic models on the formation of these units. This gradient, for example, cannot be achieved in the context of a trapped oceanic crust lying above the subduction zone. This oceanic crust generally escapes subduction and is deformed only during continental collision [92–94], for which a higher geothermal gradient should be expected. Our data do not support a Late Cretaceous–Early Tertiary deformation of the IL Units in an intraoceanic transpressional setting during the closure of the Ligure–Piemontese oceanic basin, as proposed for the ophiolite-bearing units of Southern Tuscany by [47]. This interpretation is at odds with the P – T conditions estimated in this study as well as with the deformation features detected in the Palombini Shale Fm.

The only geodynamic setting where the estimated cold geothermal gradient can occur is a subduction zone [95–98]. Moreover, the P conditions are not compatible with a D1 phase developed in a subduction setting by frontal accretion because this mechanism implies a deformation that occurs at a depth shallower than 8–10 km [99–102]. The estimated P – T conditions and the structural features of the D1 phase are instead coherent with a process of underplating at different structural levels at the base of the accretionary wedge. According to the lack of evidence of tectonic mélanges in all the IL Units, the transfer within the accretionary wedge clearly occurred via coherent underplating as proposed by [24,28,29]. So, the IL Units can be interpreted as fragments of the Ligure–Piemontese oceanic basin involved in a subduction zone via underplating before the Oligocene.

This interpretation allows some considerations about the correlation of the IL Units with the ophiolite units of Ligurian Alps, i.e., the Voltri Massif. The IL Units are separated from the Voltri Massif by the Sestri Voltaggio line that has been classically interpreted as the Alps–Apennines boundary [103–107]. Along this line, in fact, a sharp metamorphic gap is recorded with the high-pressure Voltri Massif, deeply involved in Alpine subduction, tectonically detached from the lower grade IL Units east of the Sestri–Voltaggio line and lacking a subduction signature related to Alpine history. The data provided in this paper indicate that the Palombini Shale Fm., far east of the Sestri–Voltaggio line, is also affected by metamorphism ascribable to low blueschists facies conditions. In addition, low blueschists facies metamorphic conditions within the IL Units have been reported just east of the Sestri–Voltaggio line [55] and at the top of the Voltri Massif, i.e., in the Montenotte [108] and the Moglio–Testico [82] Units. A similar setting can be also envisaged for the ophiolitic units of the Western Alps, where two types of contrasting tectono-metamorphic evolutions have been detected [109]. The structurally lower ophiolite-bearing units [e.g., the Zermatt–Saas Fee Unit] show a predominance of ophiolites over metasediments and are characterized by an eclogite metamorphic imprint [98] with local ultra- HP relics [110]. The structurally upper ophiolite-bearing unit [e.g., the Combin zone] is instead dominated by metasediments with greenschist facies paragenesis overprinted on blueschist facies relics [111].

A new scenario for the Alps–Apennines junction area can thus be proposed. Both the Apennine and Alpine ophiolite-bearing units are not only derived from the same oceanic basin but also share the same subduction-related metamorphism. Therefore, we can infer here that the two groups of units were part of the same pre-Oligocene Alpine accretionary wedge. In this scenario, the IL Units were deformed during underplating at shallow to moderate levels [28], whereas the eclogite facies metamorphic ophiolites of the Voltri Massif and Zermatt–Saas Fee Unit represent an episode of subduction at much deeper levels [112].

8. Conclusions

The data collected in this paper allow for the reviewing of the P – T conditions experienced by the IL Units during the pre-Oligocene peak metamorphism related to the D1 deformation phase. These conditions are estimated based on the composition of white mica and chlorite, which are assumed to be in chemical equilibrium formed during the D1 phase, by using several geothermometers and geobarometers. The results indicate that the metamorphic peak occurred at the prehnite–pumpellyite facies of P – T conditions for the Bracco–Val Graveglia and Colli–Tavarone Units and at the low blueschists facies conditions

for the Portello and Gottero Units. This finding indicates that a P increase during the D1 phase occurred between the first and the second group of IL Units. In addition, the collected data clearly indicate a geothermal gradient during the D1 phase of about 7–15 °C/Km that allows the consideration of the IL Units as fragments of oceanic lithosphere deformed during the closure of the Ligure-Piemontese oceanic basin via coherent underplating to an accretionary wedge at a depth ranging from 13 to 35 km. This interpretation provides further evidence of the strict correlation between the ophiolite units of the Alps and the IL Units. This correlation confirms that these two groups of units belonged to the same Alpine accretionary wedge originated during the Late Cretaceous–Oligocene closure of the Ligure-Piemontese oceanic basin.

Supplementary Materials: The following supporting information can be downloaded at: <https://www.mdpi.com/article/10.3390/min14010064/s1>. Supplementary Material: Analytical condition [113]; Table S1: mineral chemistry of white mica; Table S2: minerals chemistry of chlorite; Table S3: parameters of the chlorite-quartz-water method; Figure S1: results of the phengite-quartz-water method; Figure S2: results of the chlorite-phengite-quartz-water method.

Author Contributions: Conceptualization, M.D.R., E.S., M.M., F.M. and L.P.; methodology, E.S. and M.D.R.; software, E.S. and M.D.R.; validation, M.D.R., E.S., M.M., F.M. and L.P.; formal analysis, E.S. and M.D.R.; investigation, M.M., F.M. and L.P.; resources, M.M. and F.M.; data curation, E.S. and M.D.R.; writing—original draft preparation, M.D.R., E.S. and M.M.; writing—review and editing, M.D.R., E.S., M.M., F.M. and L.P.; visualization, E.S. and M.D.R.; supervision, M.M., F.M. and L.P.; project administration, E.S. and L.P.; funding acquisition, M.M. and F.M. All authors have read and agreed to the published version of the manuscript.

Funding: The project was supported by the University of Pisa (PRA project to Francesca Meneghini and ATENEO grant) and by the Italian Ministry of University and Research (PRIN project 2020).

Data Availability Statement: The data presented in this study are available on request from the corresponding author.

Acknowledgments: We extend our sincere thanks to the reviewers for their constructive and thorough reviews, from which we have benefited greatly in revising our manuscript.

Conflicts of Interest: The authors declare no conflicts of interest.

References

1. Dilek, Y.; Furnes, H. Ophiolites and their origins. *Elements* **2014**, *10*, 93–100. [[CrossRef](#)]
2. Agard, P.; Plunder, A.; Angiboust, S.; Bonnet, G.; Ruh, J. The subduction plate interface: Rock record and mechanical coupling (from long to short timescales). *Lithos* **2018**, *320*, 537–566. [[CrossRef](#)]
3. Decandia, F.A.; Elter, P. La zona ofiolitifera del Bracco nel settore compreso tra Levante e la Val Graveglia (Appennino Ligure). *Mem. Soc. Geol. It.* **1972**, *11*, 503–530.
4. Abbate, E.; Bortolotti, V.; Conti, M. Apennines and Alps ophiolites and the evolution of the Western Tethys. *Mem. Soc. Geol. It.* **1986**, *31*, 23–44.
5. Bortolotti, V.; Principi, G.; Treves, B. Ophiolites, Ligurides and the tectonic evolution from spreading to convergence of a Mesozoic Western Tethys segment. In *Anatomy of an Orogen: The Apennines and Adjacent Mediterranean Basins*; Springer: Dordrecht, The Netherlands, 2001; pp. 151–164.
6. Principi, G.; Bortolotti, V.; Chiari, M.; Cortesogno, L.; Gaggero, L.; Marcucci, M.; Sacconi, E.; Treves, B. The pre-orogenic volcano-sedimentary covers of the western Tethys oceanic basin: A review. *Ophioliti* **2004**, *29*, 177–212.
7. Boccaletti, M.; Elter, P.; Guazzone, G. Plate tectonic models for the development of the Western Alps and Northern Apennines. *Nat. Phys. Sci.* **1971**, *234*, 108–111. [[CrossRef](#)]
8. Elter, P.; Pertusati, P.C. Considerazioni sul limite Alpi-Appennino e sulle relazioni con l'arco delle Alpi Occidentali. *Mem. Soc. Geol. It.* **1973**, *12*, 359–375.
9. Principi, G.; Treves, B. Il sistema Corso-Appennino come prisma di accrezione. Riflessi sul problema generale del limite Alpi-Appennino. *Mem. Soc. Geol. It.* **1984**, *28*, 529–576.
10. Bortolotti, V.; Principi, G.; Treves, B. Mesozoic evolution of Western Tethys and the Europe/Iberia/Adria plate junction. *Mem. Soc. Geol. It.* **1990**, *45*, 393–407.
11. Doglioni, C. A proposal of kinematic modelling for W-dipping subductions-possible applications to the Tyrrhenian–Apennines system. *Terra Nova* **1991**, *3*, 423–434. [[CrossRef](#)]

12. Malavieille, J.; Chemenda, A.; Larroque, C. Evolutionary model for Alpine Corsica: Mechanism for ophiolite emplacement and exhumation of high-pressure rocks. *Terra Nova* **1998**, *10*, 317–322. [[CrossRef](#)]
13. Molli, G. Northern Apennines-Corsica orogenic system: An updated overview. *Geol. Soc. Lond. Spec. Publ.* **2008**, *298*, 413–442. [[CrossRef](#)]
14. Argnani, A. Plate motion and the evolution of Alpine Corsica and Northern Apennines. *Tectonophysics* **2012**, *579*, 207–219. [[CrossRef](#)]
15. Cortesogno, L.; Galbiati, B.; Principi, G. Note alla “Carta geologica delle ofioliti del Bracco” e ricostruzione della paleogeografia giurassico-cretacea. *Ofioliti* **1987**, *12*, 261–342.
16. Marroni, M.; Meccheri, M. L’Unità di Colli/Tavarone in Alta Val di Vara (Appennino Ligure): Caratteristiche litostratigrafiche e assetto strutturale. *Boll. Soc. Geol. It.* **1993**, *112*, 781–798.
17. Molli, G. Pre-orogenic tectonic framework of the northern Apennines ophiolites. *Eclogae Geol. Helv.* **1996**, *89*, 163–180.
18. Decarlis, A.; Gillard, M.; Tribuzio, R.; Epin, M.E.; Manatschal, G. Breaking up continents at magma-poor rifted margins: A seismic v. outcrop perspective. *J. Geol. Soc.* **2018**, *175*, 875–882. [[CrossRef](#)]
19. Festa, A.; Meneghini, F.; Balestro, G.; Pandolfi, L.; Tartarotti, P.; Dilek, Y.; Marroni, M. Comparative analysis of the sedimentary cover units of the Jurassic Western Tethys ophiolites in the Northern Apennines and Western Alps (Italy): Processes of the formation of mass-transport and chaotic deposits during seafloor spreading and subduction zone tectonics. *J. Geol.* **2021**, *129*, 533–561.
20. Pertusati, P.C.; Horremberger, J.C. Studio strutturale degli Scisti della Val Lavagna (Unità del Gottero, Appennino ligure). *Boll. Soc. Geol. It.* **1975**, *94*, 1375–1436.
21. Meccheri, M.; Antompaoli, M.L. Analisi strutturale ed evoluzione delle deformazioni della regione di M. Verruga, M. Porcile e Maissana (Appennino Ligure, La Spezia). *Boll. Soc. Geol. It.* **1982**, *101*, 117–140.
22. Van Zupthen, A.C.A.; van Wamel, W.A.; Bons, A.J. The structure of the Val Lavagna Nappe in the region of the Monte Ramaceto and Val Graveglia (Ligurian Apennines, Italy). *Geol. Mijnb.* **1985**, *64*, 373–384.
23. Van Wamel, W.A. On the tectonics of the Ligurian Apennines (northern Italy). *Tectonophysics* **1987**, *142*, 87–98. [[CrossRef](#)]
24. Marroni, M. Deformation history of the Mt. Gottero Unit (Internal Liguride Units, Northern Apennines). *Boll. Soc. Geol. It.* **1991**, *110*, 727–736.
25. Hoogerduijn Strating, E.H.; Van Wamel, W.A. The structure of the Bracco complex (Ligurian Apennines, Italy): A change from Alpine to Apennine polarity. *J. Geol. Soc. Lond.* **1989**, *146*, 933–944. [[CrossRef](#)]
26. Hoogerduijn Strating, E.H. Extensional faulting in an intraoceanic subduction complex—Working hypothesis for the Paleogene of the Alps-Apennine system. *Tectonophysics* **1994**, *238*, 255–273. [[CrossRef](#)]
27. Marroni, M.; Meneghini, F.; Pandolfi, L. A revised subduction inception model to explain the Late Cretaceous, double-vergent orogen in the precollisional western Tethys: Evidence from the Northern Apennines. *Tectonics* **2017**, *36*, 2227–2249. [[CrossRef](#)]
28. Meneghini, F.; Marroni, M.; Pandolfi, L. Fluid flow during accretion in sediment-dominated margins: Evidence of a high-permeability fossil fault zone from the Internal Ligurian accretionary units of the Northern Apennines, Italy. *J. Struct. Geol.* **2007**, *29*, 515–529. [[CrossRef](#)]
29. Meneghini, F.; Pandolfi, L.; Marroni, M. Recycling of heterogeneous material in the subduction factory: Evidence from the sedimentary mélange of the Internal Ligurian Units, Italy. *J. Geol. Soc.* **2020**, *177*, 587–599. [[CrossRef](#)]
30. Venturelli, G.; Frey, M. Anchizone metamorphism in sedimentary sequences of the Northern Apennines. *Rend. Soc. It. Miner. Petrol.* **1977**, *33*, 109–123.
31. Bonazzi, A.; Cortesogno, L.; Galbiati, B.; Reinhardt, M.; Salvioli Mariani, E.; Vernia, L. Nuovi dati sul metamorfismo di basso grado nelle unità Liguridi interne e loro possibile significato nell’evoluzione strutturale dell’Appennino Settentrionale. *Acta Nat. At. Parm.* **1987**, *23*, 17–47.
32. Molli, G.; Pandolfi, L.; Tamponi, M. «Cristallinità» di illite e clorite nelle Unità Liguri dell’Alta Val Trebbia (Appennino Settentrionale). *Atti Soc. Toscana Sci. Nat.* **1992**, *99*, 79–92.
33. Reinhardt, M. Vitrinite reflectance, illite crystallinity and tectonics: Results from the Northern Apennines (Italy). *Org. Geochem.* **1991**, *17*, 175–184.41. [[CrossRef](#)]
34. Ducci, M.; Leoni, L.; Marroni, M.; Tamponi, M. Determinazione del grado metamorfico dell’Unità Gottero in alta Val Lavagna (Liguria Orientale, Appennino Settentrionale). *Atti Soc. Toscana Sci. Nat.* **1995**, *102*, 39–46.
35. Leoni, L.; Marroni, M.; Sartori, F.; Tamponi, M. Indicators of very-low grade metamorphism in metapelites from Bracco/Val Graveglia Unit (Ligurian Apennines, Northern Italy) and their relationships with deformation. *Acta Vulc. Mar. Vol.* **1992**, *2*, 277–285.
36. Leoni, L.; Marroni, M.; Sartori, F.; Tamponi, M. Metamorphic grade in metapelites of the internal liguride units (Northern Apennines, Italy). *Eur. J. Mineral.* **1996**, *8*, 35–50. [[CrossRef](#)]
37. Ellero, A.; Leoni, L.; Marroni, M.; Sartori, F. Internal Liguride Units from Central Liguria, Italy: New constraints to the tectonic setting from white mica and chlorite studies. *Schweiz. Mineral. Petrogr. Mitteilungen* **2001**, *81*, 39–53.
38. Reutter, K.-J.; Teichmüller, M.; Teichmüller, R.; Zanzucchi, G. The coalification pattern in the Northern Apennines and its paleogeothermic and tectonic significance. *Geol. Rund.* **1983**, *72*, 861–894. [[CrossRef](#)]

39. Malavieille, J.; Molli, G.; Genti, M.; Dominguez, S.; Beyssac, O.; Taboada, A.; Vitale-Borvarone, A.; Lu, C.-Y.; Chen, C.-T. Formation of ophiolite-bearing tectono-sedimentary mélanges in accretionary wedges by gravity driven submarine erosion: Insights from analog models and case studies. *J. Geodyn.* **2016**, *100*, 87–103. [[CrossRef](#)]
40. Willner, A.P. Very-low-grade metamorphism. *Encycl. Geol.* **2021**, *2*, 513–521.
41. Frey, M.; Robinson, D. *Low-Grade Metamorphism*; John Wiley & Sons: Hoboken, NJ, USA, 2009; 328p.
42. Tinkham, D.K.; Ghent, E.D. Estimating P–T conditions of garnet growth with isochemical phase-diagram sections and the problem of effective bulk-composition. *Can. Mineral.* **2005**, *43*, 35–50. [[CrossRef](#)]
43. Plunder, A.; Agard, P.; Dubacq, B.; Chopin, C.; Bellanger, M. How continuous and precise is the record of P–T paths? Insights from combined thermobarometry and thermodynamic modelling into subduction dynamics (Schistes Lustrés, W. Alps). *J. Metam. Geol.* **2012**, *30*, 323–346. [[CrossRef](#)]
44. Lanari, P.; Engi, M. Local bulk composition effects on metamorphic mineral assemblages. *Rev. Mineral. Geochem.* **2017**, *83*, 55–102. [[CrossRef](#)]
45. Lanari, P.; Duesterhoeft, E. Modeling metamorphic rocks using equilibrium thermodynamics and internally consistent databases: Past achievements, problems and perspectives. *J. Petrol.* **2019**, *60*, 19–56. [[CrossRef](#)]
46. Treves, B. Orogenic belts as accretionary prisms: The example of the northern Apennines. *Ofioliti* **1984**, *9*, 577–618.
47. Nirta, G.; Principi, G.; Vannucchi, P. The Ligurian Units of Western Tuscany (Northern Apennines): Insight on the influence of pre-existing weakness zones during ocean closure. *Geod. Acta* **2007**, *20*, 71–97. [[CrossRef](#)]
48. Meneghini, F.; Di Rosa, M.; Marroni, M.; Raimbourg, H.; Pandolfi, L. Subduction signature in the Internal Ligurian Units (Northern Apennine, Italy): Evidence from P–T metamorphic peak estimate. *Terra Nova* **2023**. [[CrossRef](#)]
49. Berman, R.G. Thermobarometry using multi-equilibrium calculations; a new technique, with petrological applications. *Can. Mineral.* **1991**, *29*, 833–855.
50. Elter, P. L'ensemble ligure. *Bull. Soc. Géol. Fr.* **1975**, *7*, 984–997. [[CrossRef](#)]
51. Mantovani, F.; Elter, F.M.; Pandeli, E.; Briguglio, A.; Piazza, M. The Portofino Conglomerate (Eastern Liguria, Northern Italy): Provenance, Age and Geodynamic Implications. *Geosciences* **2023**, *13*, 154. [[CrossRef](#)]
52. Costa, E.; Di Giulio, A.; Villa, G. La finestra tettonica di Monte Zuccone (Appennino settentrionale): Rilevamento, petrografia delle arenarie e biostratigrafia. *Atti Tic. Sci. Terra.* **1989**, *32*, 175–190.
53. Elter, P.; Catanzariti, R.; Ghiselli, F.; Marroni, M.; Molli, G.; Ottria, G.; Pandolfi, L. L'unità Aveto (Appennino Settentrionale): Caratteristiche litostratigrafiche, biostratigrafia, petrografia delle arenite ed assetto strutturale. *Boll. Soc. Geol. It.* **1999**, *118*, 41–64.
54. Di Rosa, M.; Frassi, C.; Malasoma, A.; Marroni, M.; Meneghini, F.; Pandolfi, L. Syn-exhumation coupling of oceanic and continental units along the western edge of the Alpine Corsica: A review. *Ofioliti* **2020**, *45*, 71–102.
55. Capponi, G.; Crispini, L.; Federico, L.; Malatesta, C. Geology of the Eastern Ligurian Alps: A review of the tectonic units. *It. J. Geos.* **2016**, *135*, 157–169. [[CrossRef](#)]
56. Federico, L.; Capponi, G.; Crispini, L.; Scambelluri, M.; Villa, I.M. ³⁹Ar/⁴⁰Ar dating of high-pressure rocks from the Ligurian Alps: Evidence for a continuous subduction–exhumation cycle. *Earth Planet. Sci. Lett.* **2005**, *240*, 668–680. [[CrossRef](#)]
57. Elter, P.; Marroni, M.; Molli, G.; Pandolfi, L. Caratteristiche stratigrafiche del Complesso di M.Penna/Casanova (Val Trebbia, Appennino Settentrionale). *Atti Tic. Sci. Ter.* **1991**, *34*, 97–106.
58. Marroni, M.; Meneghini, F.; Pandolfi, L.; Noah, H.; Luvisi, E. The Ottone-Levanto Line of Eastern Liguria (Italy) uncovered: A Late Eocene-Early Oligocene snapshot of Northern Apennine geodynamics at the Alps/Apennines Junction. *Episodes* **2019**, *42*, 107–118. [[CrossRef](#)]
59. Ducci, M.; Lazzaroni, F.; Marroni, M.; Pandolfi, L.; Taini, A. Tectonic framework of the northern Ligurian Apennine, Italy. *C. R. Acad. Sci. Paris* **1997**, *324*, 317–324.
60. Bortolotti, V.; Principi, G. The Bargonasco-Upper Val Graveglia ophiolitic succession, Northern Apennines, Italy. *Ofioliti* **2003**, *28*, 137–140.
61. Fonesu, M.; Felletti, F. Facies and architecture of a sand-rich turbidite system in an evolving collisional-trench basin: A case history from the Upper Cretaceous-Palaeocene Gottero System (NW Apennines). *Riv. Ital. Paleontol. Stratigr.* **2019**, *125*, 449–487.
62. Marroni, M.; Monechi, S.; Perilli, N.; Principi, G.; Treves, B. Cretaceous flysch deposits of the Northern Apennines, Italy: Age of inception of orogenesis-controlled sedimentation. *Cretac. Res.* **1992**, *13*, 487–504. [[CrossRef](#)]
63. Di Biase, D.; Marroni, M.; Pandolfi, L. Age of the deformation phases in the Internal Liguride units: Evidences from lower Oligocene Val Borbera Conglomerates of Tertiary Piedmont Basin (northern Italy). *Ofioliti* **1997**, *22*, 231–238.
64. Ramsay, J.G. *Folding and Fracturing of Rocks*; Mc Graw Hill Book Company: New York, NY, USA, 2011; p. 568.
65. Cortesogno, L.; Haccard, D. Note illustrative alla Carta Geologica della zona Sestri-Voltaggio. *Mem. Soc. Geol. It.* **1984**, *28*, 115–150.
66. Crispini, L.; Capponi, G. Tectonic evolution of the Voltri Massif and Sestri Voltaggio Zone (southern limit of the NW Alps): A review. *Ofioliti* **2001**, *26*, 161–164.
67. Lucchetti, G.; Cabella, R.; Cortesogno, L. Pumpellyites and coexisting minerals in different low-grade metamorphic facies of Liguria, Italy. *J. Metamorph. Geol.* **1990**, *8*, 539–550. [[CrossRef](#)]
68. Balestrieri, M.L.; Abbate, E.; Bigazzi, G. Insights on the thermal evolution of the Ligurian Apennines (Italy) through fission-track analyses. *J. Geol. Soc. Lond.* **1996**, *153*, 419–425. [[CrossRef](#)]

69. Rahn, M.; Brandon, M.T.; Batt, G.E.; Garver, J.I. A zero-damage model for fission-track annealing in zircon. *Am. Mineral.* **2004**, *89*, 473–484. [[CrossRef](#)]
70. Burkhard, M. Calcite twins, their geometry, appearance and significance as stress-strain markers and indicators of tectonic regime: A review. *J. Struct. Geol.* **1993**, *15*, 351–368. [[CrossRef](#)]
71. Ferrill, D.A.; Morris, A.P.; Evans, M.A.; Burkhard, M.; Groshong, R.H., Jr.; Onasch, C.M. Calcite twin morphology: A low-temperature deformation geothermometer. *J. Struct. Geol.* **2004**, *26*, 1521–1529. [[CrossRef](#)]
72. De Andrade, V.; Vidal, O.; Lewin, E.; O'Brien, P.; Agard, P. Quantification of electron microprobe compositional maps of rock thin sections: An optimized method and examples. *J. Met. Geol.* **2006**, *24*, 655–668. [[CrossRef](#)]
73. Lanari, P.; Vidal, O.; De Andrade, V.; Dubacq, B.; Lewin, E.; Grosch, E.; Schwartz, S. XMAPTOOLS: A MATLAB c-based program for electron microprobe X-ray image processing and geothermobarometry. *Comput. Geosci.* **2014**, *62*, 227–240. [[CrossRef](#)]
74. Cathelineau, M. Cation site occupancy in chlorites and illites as a function of temperature. *Clay Mineral.* **1988**, *23*, 471–485. [[CrossRef](#)]
75. Lanari, P.; Wagner, T.; Vidal, O. A thermodynamic model for di-trioctahedral chlorite from experimental and natural data in the system MgO-FeO-Al₂O₃-SiO₂-H₂O: Applications to P–T sections and geothermometry. *Contrib. Mineral. Petrol.* **2014**, *167*, 968. [[CrossRef](#)]
76. Bourdelle, F.; Parra, T.; Chopin, C.; Beyssac, O. A new chlorite geothermometer for diagenetic to low-grade metamorphic conditions. *Contrib. Mineral. Petrol.* **2013**, *165*, 723–735. [[CrossRef](#)]
77. Massonne, H.J.; Schreyer, W. Phengite geobarometry based on the limiting assemblage with K-feldspar, phlogopite, and quartz. *Contrib. Mineral. Petrol.* **1987**, *96*, 212–224. [[CrossRef](#)]
78. Vidal, O.; De Andrade, V.; Lewin, E.; Munoz, M.; Parra, T.; Pascarelli, S. P–T deformation Fe²⁺/Fe³⁺ mapping at the thin section scale and comparison with XANES mapping: Application to a garnet-bearing metapelite from the Sambagawa metamorphic belt (Japan). *J. Met. Geol.* **2006**, *24*, 669–683. [[CrossRef](#)]
79. Dubacq, B.; Vidal, O.; De Andrade, V. Dehydration of dioctahedral aluminous phyllosilicates: Thermodynamic modelling and implications for thermobarometric estimates. *Contrib. Mineral. Petrol.* **2010**, *159*, 159–174. [[CrossRef](#)]
80. Vidal, O.; Parra, T. Exhumation paths of high-pressure metapelites obtained from local equilibria for chlorite-phengite assemblage. *Geol. J.* **2000**, *35*, 139–161. [[CrossRef](#)]
81. Di Rosa, M.; Meneghini, F.; Marroni, M.; Frassi, C.; Pandolfi, L. The coupling of high-pressure oceanic and continental units in Alpine Corsica: Evidence for syn-exhumation tectonic erosion at the roof of the plate interface. *Lithos* **2020**, *354*, 105328. [[CrossRef](#)]
82. Sanità, E.; Di Rosa, M.; Lardeaux, J.M.; Marroni, M.; Pandolfi, L. The Moglio-Testico Unit as subducted metamorphic oceanic fragments: Stratigraphic, structural and metamorphic constrains. *Minerals* **2022**, *12*, 1343. [[CrossRef](#)]
83. Guidotti, C.V.; Sassi, F.P. Constraints on studies of metamorphic K-Na white micas. *Rev. Mineral. Geochem.* **2002**, *46*, 413–448. [[CrossRef](#)]
84. Warr, L.N. IMA–CNMNC approved mineral symbols. *Mineral. Mag.* **2021**, *85*, 291–320. [[CrossRef](#)]
85. Bourdelle, F.; Cathelineau, M. Low-temperature chlorite geothermometry: A graphical representation based on a T–R₂–Si diagram. *Eur. J. Mineral.* **2015**, *27*, 617–626. [[CrossRef](#)]
86. Bucher, K.; Grapes, R. *Petrogenesis of Metamorphic Rocks*, 8th ed.; Springer: Berlin/Heidelberg, Germany, 2011; p. 428.
87. Kübler, B. Cristallinité de l'illite et mixed-layer: Brève révision. *Schweiz. Mineral. Petr. Mitt.* **1990**, *70*, 89–93.
88. Merriman, R.J.; Frey, M. Patterns of very low-grade metamorphism in metapelitic rocks. In *Low-Grade Metamorphism*; Frey, M., Robinson, D., Eds.; Blackwell Science Ltd.: Hoboken, NJ, USA, 1998; pp. 61–107.
89. Merriman, R.J.; Peacor, D.R. Very low-grade metapelites: Mineralogy, microfabrics and measuring reaction progress. In *Low-Grade Metamorphism*; Frey, M., Robinson, D., Eds.; Blackwell Science Ltd.: Hoboken, NJ, USA, 1998; pp. 10–60.
90. Mullis, J.; Stern, W.B.; Capitani, C. Correlation of fluid inclusion temperatures with illite, smectite and chlorite “crystallinity” data and smear slide chemistry in sedimentary rocks from the external parts of the Central Alps (Switzerland). In *IGCP Project 294, Low Temperature Metamorphism Symposium*; Ein Dienst der ETH-Bibliothek: Santiago de Chile, Chile, 1993.
91. Roberts, B.; Merriman, R.J.; Pratt, W. The influence of strain, lithology and stratigraphical depth on white mica (illite) crystallinity in mudrocks from the vicinity of the Corris Slate Belt, Wales: Implications for the timing of metamorphism in the Welsh Basin. *Geol. Mag.* **1991**, *128*, 633–645. [[CrossRef](#)]
92. Karig, D.E.; Sharman, G.F. Subduction and accretion in trenches. *Geol. Soc. Am. Bull.* **1975**, *86*, 377–389. [[CrossRef](#)]
93. Dickinson, W.R.; Seely, D.R. Structure and stratigraphy of forearc regions. *AAPG Bull.* **1979**, *63*, 2–31.
94. England, P.C.; Thompson, A.B. Pressure—Temperature—Time paths of regional metamorphism I. Heat transfer during the evolution of regions of thickened continental crust. *J. Petrol.* **1984**, *25*, 894–928. [[CrossRef](#)]
95. Ruh, J.B.; Le Pourhiet, L.; Agard, P.; Burov, E.; Gerya, T. Tectonic slicing of subducting oceanic crust along plate interfaces: Numerical modeling. *Geochem. Geophys. Geosyst.* **2015**, *16*, 3505–3531. [[CrossRef](#)]
96. Groppo, C.; Castelli, D. Prograde P–T evolution of a lawsonite eclogite from the Monviso meta-ophiolite (Western Alps): Dehydration and redox reactions during subduction of oceanic FeTi-oxide gabbro. *J. Petrol.* **2010**, *51*, 2489–2514. [[CrossRef](#)]
97. Angiboust, S.; Agard, P.; Yamato, P.; Raimbourg, H. Eclogite breccias in a subducted ophiolite: A record of intermediate-depth earthquakes? *Geology* **2012**, *40*, 707–710. [[CrossRef](#)]

98. Ghignone, S.; Sudo, M.; Balestro, G.; Borghi, A.; Gattiglio, M.; Ferrero, S.; Van Schijndel, V. Timing of exhumation of meta-ophiolite units in the Western Alps: New tectonic implications from $40\text{Ar}/39\text{Ar}$ white mica ages from Piedmont Zone (Susa Valley). *Lithos* **2021**, *404*, 106443. [[CrossRef](#)]
99. Moore, J.C.; Cowan, D.S.; Karig, D.E. Structural styles and deformation fabrics of accretionary complexes. *Geology* **1985**, *13*, 77–79. [[CrossRef](#)]
100. Von Huene, R.; Scholl, D.W. Observations at convergent margins concerning sediment subduction, subduction erosion, and the growth of continental crust. *Rev. Geophys.* **1991**, *29*, 279–316. [[CrossRef](#)]
101. Lallemand, S.E.; Schnürle, P.; Malavieille, J. Coulomb theory applied to accretionary and nonaccretionary wedges: Possible causes for tectonic erosion and/or frontal accretion. *Journal of Geophysical Research. Solid Earth*. **1994**, *99*, 12033–12055.
102. Fagereng, Å.; Savage, H.M.; Morgan, J.K.; Wang, M.; Meneghini, F.; Barnes, P.M.; Bell, R.; Kitajima, H.; McNamara, D.D.; Saffer, D.M.; et al. Mixed deformation styles observed on a shallow subduction thrust, Hikurangi margin, New Zealand. *Geology* **2019**, *47*, 872–876. [[CrossRef](#)]
103. Scholle, P.A. Diagenesis of deep-water carbonate turbidites, upper Cretaceous Monte Antola flysch, northern Apennines, Italy. *J. Sedim. Res.* **1971**, *41*, 233–250.
104. Gelati, R.; Pasquaré, G. Interpretazione geologica del limite Alpi–Appennini in Liguria. *Riv. It. Paleont.* **1970**, *76*, 513–578.
105. Vanossi, M.; Cortesogno, L.; Galbiati, B.; Messiga, B.; Piccardo, G.B.; Vannucci, R. Geologia delle Alpi liguri: Dati, problemi, ipotesi. *Mem. Soc. Geol. It.* **1986**, *28*, 5–75.
106. Castellarin, A. Alps–Apennines and Po plain–frontal Apennines relations. In *Anatomy of an Orogen: The Apennines and Adjacent Mediterranean Basins*; Springer: Dordrecht, The Netherlands, 2001; pp. 117–195.
107. Mosca, P.; Polino, R.; Rogledi, S.; Rossi, M. New data for the kinematic interpretation of the Alps–Apennines junction (Northwestern Italy). *Int. J. Earth Sci.* **2010**, *99*, 833–849. [[CrossRef](#)]
108. Seno, S.; Dallagiovanna, G.; Vanossi, M. A kinematic evolutionary model for the Penninic sector of the central Ligurian Alps. *Int. J. Earth Sci.* **2005**, *94*, 114–129. [[CrossRef](#)]
109. Negro, F.; Bousquet, R.; Vils, F.; Pellet, C.M.; Hänggi-Schaub, J. Thermal structure and metamorphic evolution of the Piemont–Ligurian metasediments in the northern Western Alps. *Swiss J. Geo.* **2013**, *106*, 63–78. [[CrossRef](#)]
110. Frezzotti, M.L.; Palmeri, R.; Godard, G.; Ferrando, S.; Compagnoni, R. A Dynamic Pressure Component in UHP Whiteschists from the Dora-Maira Massif (Western Alps, Italy) Revealed by Pressure-Induced Incipient Amorphization of Quartz. In *Proceedings of the AGU Fall Meeting, San Francisco, CA, USA, 15–19 December 2014*; p. V13B-4781.
111. Manzotti, P.; Ballèvre, M.; Pitra, P.; Schiavi, F. Missing lawsonite and aragonite found: P–T and fluid composition in meta-marls from the Combin Zone (Western Alps). *Contrib. Mineral. Petrol.* **2021**, *176*, 60. [[CrossRef](#)]
112. Malatesta, C.; Gerya, T.; Scambelluri, M.; Federico, L.; Crispini, L.; Capponi, G. Intraoceanic subduction of “heterogeneous” oceanic lithosphere in narrow basins: 2D numerical modeling. *Lithos* **2012**, *140*, 234–251. [[CrossRef](#)]
113. Lanari, P. Micro-cartographie P–T–t dans les Roches Métamorphiques. Applications aux Alpes et à l’Himalaya. Ph.D. Thesis, Université de Grenoble, Grenoble, France, 2012.

Disclaimer/Publisher’s Note: The statements, opinions and data contained in all publications are solely those of the individual author(s) and contributor(s) and not of MDPI and/or the editor(s). MDPI and/or the editor(s) disclaim responsibility for any injury to people or property resulting from any ideas, methods, instructions or products referred to in the content.